Reactivity of nitric oxide with the [4Fe–4S] cluster of dihydroxyacid dehydratase from *Escherichia coli*

Xuewu DUAN, Juanjuan YANG, Binbin REN, Guoqiang TAN and Huangen DING[1]

Department of Biological Sciences, Louisiana State University, Baton Rouge, LA 70803, U.S.A.

Although the NO (nitric oxide)-mediated modification of iron–sulfur proteins has been well-documented in bacteria and mammalian cells, specific reactivity of NO with iron–sulfur proteins still remains elusive. In the present study, we report the first kinetic characterization of the reaction between NO and iron–sulfur clusters in protein using the *Escherichia coli* IlvD (dihydroxyacid dehydratase) [4Fe–4S] cluster as an example. Combining a sensitive NO electrode with EPR (electron paramagnetic resonance) spectroscopy and an enzyme activity assay, we demonstrate that NO is rapidly consumed by the IlvD [4Fe–4S] cluster with the concomitant formation of the IlvD-bound DNIC (dinitrosyl–iron complex) and inactivation of the enzyme activity under anaerobic conditions. The rate constant for the initial reaction between NO and the IlvD [4Fe–4S] cluster is estimated to be $(7.0 \pm 2.0) \times 10^6$ $M^{-2} \cdot s^{-1}$ at 25 °C, which is approx. 2–3 times faster than that of the NO autoxidation by O_2 in aqueous solution. Addition of GSH failed to prevent the NO-mediated modification of the IlvD [4Fe–4S] cluster regardless of the presence of O_2 in the medium, further suggesting that NO is more reactive with the IlvD [4Fe–4S] cluster than with GSH or O_2. Purified aconitase B [4Fe–4S] cluster from *E. coli* has an almost identical NO reactivity as the IlvD [4Fe–4S] cluster. However, the reaction between NO and the endonuclease III [4Fe–4S] cluster is relatively slow, apparently because the [4Fe–4S] cluster in endonuclease III is less accessible to solvent than those in IlvD and aconitase B. When *E. coli* cells containing recombinant IlvD, aconitase B or endonuclease III are exposed to NO using the Silastic tubing NO delivery system under aerobic and anaerobic conditions, the [4Fe–4S] clusters in IlvD and aconitase B, but not in endonuclease III, are efficiently modified forming the protein-bound DNICs, confirming that NO has a higher reactivity with the [4Fe–4S] clusters in IlvD and aconitase B than with O_2 or GSH. The results suggest that the iron–sulfur clusters in proteins such as IlvD and aconitase B may constitute the primary targets of the NO cytotoxicity under both aerobic and anaerobic conditions.

Key words: dihydroxyacid dehydratase, dinitrosyl–iron complex, iron–sulfur protein, nitric oxide.

INTRODUCTION

In biological systems, NO (nitric oxide) has a relatively short half-life time (in the order of 2 ms to 2 s) primarily due to autoxidation by O_2 [1–3]. The reaction between NO and O_2 in aqueous solution occurs in the following equation (eqn 1):

$$4NO + O_2 + 2H_2O \rightarrow 4H^+ + 4NO_2^- \quad \text{(eqn 1)}$$

The rate constant for NO autoxidation in aqueous solution is approx. 2.0×10^6 $M^{-2} \cdot s^{-1}$ at 25 °C [3,4]. NO autoxidation can be further accelerated by approx. 300-fold in biological membranes where both NO and O_2 are concentrated via partitioning [4,5]. Conceivably, the rapid NO autoxidation by O_2 could limit the NO availability as a signalling molecule for intercellular communications [6] and as a cytotoxic weapon to kill pathogenic bacteria and tumour cells [7–9]. Nevertheless, the binding of NO to the ferrous haem in soluble guanylate cyclase is only limited by the diffusion rate of NO to the haem pocket with $k_{on} > 10^7$ $M^{-1} \cdot s^{-1}$ [10,11] and $k_{off} < 10^{-3}$ s^{-1}[11]. Such a tight binding of NO to haems would almost guarantee NO signalling even in the presence of O_2 in medium. In mitochondria, NO has also been shown to compete with O_2 for binding in the binuclear haem a_3/Cu_B centre in cytochrome *c* oxidase [12], and reversibly inhibit the respiratory electron transfer chain at submicromolar concentrations [13,14].

Another major cellular target of NO is a group of proteins that contain iron–sulfur clusters [15]. Iron–sulfur proteins have been found in diverse physiological processes such as energy conversion, sugar metabolism, amino acid biosynthesis, haem and biotin biosynthesis, RNA modification, DNA synthesis and repair, and the regulation of gene expression [16]. The NO-mediated modification of iron–sulfur proteins was first reported in the bacterium *Clostridium botulinum* [17]. When *C. botulinum* cells were exposed to NO by incubation with nitrite and ascorbate, the original EPR (electron paramagnetic resonance) signal at $g = 1.94$ of the intact iron–sulfur proteins in cells was lost and replaced with a new EPR signal at $g = 2.04$ of the protein-bound DNIC (dinitrosyl–iron complex) [17]. Later on, the same EPR signal at $g = 2.04$ was observed in activated macrophages where NO was produced by iNOS [inducible NOS (NO synthase)] [18], in tumour cells co-cultured with activated macrophages [19], in the post-operative-day-4 allografts [20], and in the gastro-oesophageal junction where NO was produced luminally from nitrite [21]. Formation of the protein-bound DNIC by NO has since been directly demonstrated in a number of iron–sulfur proteins *in vitro* [22–28]. However, the identity of the EPR signals at $g = 2.04$ observed in cells was challenged by the observations that small molecule thiols can also form the DNICs with ferrous iron and NO *in vitro* [29–31]. Nevertheless, existence of the small molecule thiol-bound DNICs has never been demonstrated in living cells [32,33], apparently because the small molecule thiol-bound DNICs are not stable in aqueous solution (e.g. the life time of the cysteine-bound DNIC is less than 1 min) [29]. The only stable glutathione-bound DNICs found in cells are associated with GSTs (glutathione transferases), a potential protection mechanism against excess NO [33]. To examine whether the iron–sulfur

Abbreviations used: DNIC, dinitrosyl–iron complex; EPR, electron paramagnetic resonance; IlvD, dihydroxyacid dehydratase; NO, nitric oxide.

[1] To whom correspondence should be addressed (email hding@lsu.edu).

proteins are actually modified forming the protein-bound DNICs by NO *in vivo*, we used the recombinant iron–sulfur proteins (the redox transcript factor SoxR [2Fe–2S] cluster [26], the ferredoxin [2Fe–2S] cluster [28] and the endonuclease III [4Fe–4S] cluster [25]) as examples, and demonstrated that these iron–sulfur proteins are converted into the protein-bound DNICs when *Escherichia coli* cells are exposed to NO under anaerobic conditions. Thus the NO-mediated modification of iron–sulfur proteins, at least in part, contributes to the observed EPR signal at $g = 2.04$ in the NO-exposed *E. coli* cells [26].

The reaction between NO and iron–sulfur clusters in proteins may be described in a following simple equation (eqn 2):

$$2NO + [Fe{-}S] \rightarrow Fe(NO)_2 + S^{2-} \quad \text{(eqn 2)}$$

However, because iron–sulfur clusters can exist in the forms of [2Fe–2S], [3Fe–4S], [4Fe–4S] and other more complicated forms [34], it is conceivable that the reactions between NO and iron–sulfur proteins could be rather complex. At present, little is known about the redox reactions underlying the NO-mediated modification of iron–sulfur clusters in protein. In the present study, we report the first kinetic characterization for the reaction between NO and the [4Fe–4S] cluster of IlvD (dihydroxyacid dehydratase) from *E. coli*. IlvD is an essential enzyme for branched-chain amino acids biogenesis in bacteria [35,36], and has been identified as a major target of NO cytotoxicity [37,38]. Combining a sensitive NO electrode with EPR spectroscopy and an enzyme activity assay, we find that NO is rapidly consumed by the IlvD [4Fe–4S] cluster with the concomitant formation of the IlvD-bound DNIC and inactivation of the enzyme activity under anaerobic conditions. The rate constant for the initial reaction between NO and the IlvD [4Fe–4S] cluster is estimated to be $(7.0 \pm 2.0) \times 10^6\ M^{-2} \cdot s^{-1}$, which is approx. 2–3-fold faster than that of the NO autoxidation by O_2 in aqueous solution. Furthermore, we show that small molecule thiol glutathione (GSH) fails to protect the IlvD [4Fe–4S] cluster from being modified by NO under aerobic or anaerobic conditions. The physiological relevance of the NO reactivity with iron–sulfur clusters in proteins will be discussed.

EXPERIMENTAL

Measurements of NO

An NO electrode (ISO-NOP) connected to an Apollo-4000 Free Radical Analyser (World Precision Instruments) was used to continuously record the NO concentration in a sealed vial with vigorous stirring. The response time of the NO electrode was less than 5 s. The observed current of the NO electrode was linear with the NO concentration from 0 to 500 μM. An NO-releasing compound diethylamine NONOate (Cayman Chemicals) was used as the NO source. The concentration of diethylamine NONOate was determined from the absorption peak at 250 nm using an molar absorption coefficient of $6.5\ mM^{-1} \cdot cm^{-1}$. For anaerobic reactions, all solutions were degassed with pure argon gas. Pre-degassed diethylamine NONOate solution [freshly dissolved in 20 mM Tris (pH 10.5)] was first injected into a sealed vial containing 3.0 ml of pre-degassed 20 mM potassium phosphate (pH 7.4). When the NO released from diethylamine NONOate reached a plateau, a pre-degassed protein sample was injected into the sealed vial anaerobically using a gas-tight Hamilton syringe. Injection of an equal volume of pre-degassed phosphate buffer was used as a reference.

Purification of *E. coli* IlvD, aconitase B and endonuclease III

The DNA fragment encoding the gene *ilvD* was amplified from *E. coli* genomic DNA with PCR using two primers (IlvD-1, 5′-ATAGAGCTCATGCCTAAGTACCGTTCCGCCACC-3′ and IlvD-2, 5′-CGCGAATTCTTAACCCCCCAGTTTCGATTTATC-3′). The PCR product was digested with restriction enzymes SacI and EcoRI, and the digested product was ligated into an expression vector pBAD (Invitrogen). Recombinant IlvD was expressed to approx. 2 % of total cellular protein in *E. coli* by adding L-arabinose to a final concentration of 0.02 %. For preparation of IlvD with reconstituted [4Fe–4S] cluster, the cell extracts were incubated with 0.5 mM L-cysteine, 1 μM cysteine desulfurase IscS, 100 μM $Fe(NH_4)_2(SO_4)_2$ and 2 mM dithiothreitol anaerobically at 37 °C for 20 min before the protein was purified as described in [25]. The iron content analysis and EPR measurements showed that the reconstituted IlvD contained a [4Fe–4S] cluster as described previously by Flint et al. [35]. For *E. coli* aconitase B, two primers (AcnB-1, 5′-GAACCGCCATGGTAGAAGAATACC-3′ and AcnB-2, 5′-TGACTTTTTAAAGCTTAGTCTGGA-3′) were used for PCR amplification. The PCR product was digested with NcoI and HindIII and ligated into pET28b+ (Stratagene). Aconitase B was expressed in *E. coli* BL21(DE3) cells and purified as described for *E. coli* endonuclease III [25]. The purity of purified proteins was over 95 % as judged by SDS/PAGE followed by Coomassie Blue staining.

Enzyme activity assays for IlvD and aconitase B

The enzyme activity of IlvD was measured using the substrate D,L-2,3-dihydroxy-isovalerate [38].

D,L-2,3-Dihydroxy-isovalerate was synthesized according to the method of Cioffi et al. [39]. All chemical reagents used for D,L-2,3-dihydroxy-isovalerate synthesis were obtained from Sigma–Aldrich. Purified IlvD or the cell extracts containing IlvD were added to pre-incubated solutions containing 50 mM Tris (pH 8.0), 10 mM $MgCl_2$ and 10 mM D,L-2,3-dihydroxy-isovalerate at 37 °C [36]. The reaction product (oxo acids) was monitored at 240 nm using a molar absorption coefficient of $0.19\ mM^{-1} \cdot cm^{-1}$ [35]. For the aconitase B activity assay, purified protein or the cell extracts were added to pre-incubation solutions containing 50 mM Tris (pH 8.0), 10 mM $MgCl_2$ and 10 mM D,L-isocitrate at 37 °C. The reaction was monitored following the formation of *cis*-aconitate at 240 nm using a molar absorption coefficient of $3.6\ mM^{-1} \cdot cm^{-1}$ [40].

NO exposure of *E. coli* cells under aerobic and anaerobic conditions

Overnight *E. coli* cells containing recombinant iron–sulfur proteins were diluted 1:100 in freshly prepared LB (Luria–Bertani) medium and incubated at 37 °C with aeration (250 rev./min) for 3 h, followed by induction of IlvD with 0.02 % L-arabinose for 1 h. Cells were harvested and re-suspended in minimal medium to $D_{600} = 2.0$. For anaerobic NO exposure, *E. coli* cells were purged with pure argon gas for 10 min before being exposed to the Silastic tubing NO-delivery system anaerobically. NO gas was first passed through a soda-lime column to remove NO_2 and higher oxides of nitrogen before being connected to the Silastic tubing [0.635 mm × 1.1938 mm (inner diameter × outer diameter); Dow Corning] [38,41]. The length of the Silastic tubing immersed in the cell culture was adjusted such that approx. 100 nM NO per s was released to cell culture. For aerobic NO exposures, *E. coli* cells were directly exposed to the Silastic tubing NO-delivery system in an open-to-air flask under vigorous stirring.

EPR measurements of the protein-bound DNICs

The X-band EPR spectra were recorded using a Bruker model ESR-300 EPR spectrometer equipped with an Oxford Instruments 910 continuous-flow cryostat. Routine EPR conditions were: microwave frequency, 9.47 GHz; microwave power, 10.0 mW; modulation frequency, 100 kHz; modulation amplitude, 1.2 mT; sample temperature, 20 K; receive gain, 10^5. The amounts of the protein-bound DNIC were calculated from the amplitude of the EPR signal at $g = 2.04$ of the freshly prepared glutathione-bound DNIC as described in [30].

RESULTS

NO is rapidly consumed by the IlvD [4Fe–4S] cluster under anaerobic conditions

To investigate the reactivity of NO with iron–sulfur clusters in proteins, we prepared a recombinant IlvD [4Fe–4S] cluster from *E. coli* as described in the Experimental section. IlvD was chosen because its [4Fe–4S] cluster is relatively stable under aerobic conditions [35]. Figure 1(A) shows the UV–visible absorption spectra of apo-IlvD and IlvD with the [4Fe–4S] cluster. The absorption peaks at 320 nm and 411 nm represent the charge-transfer bands of the [4Fe–4S] cluster in the protein [35]. Although apo-IlvD had no detectable enzyme activity, the IlvD with the [4Fe–4S] cluster was fully active to convert 2,3-dihydroxy-isovalerate into 2-oxo-isovalerate at a rate constant of approx. 200 $M^{-1} \cdot s^{-1}$ as reported previously by Flint et al. [35].

To investigate the reaction kinetics between NO and the [4Fe–4S] cluster of IlvD, we used diethylamine NONOate as an NO donor which releases 1.5 mol of NO with a half-life time of 16 min at room temperature and pH 7.2. The NO concentration in a pre-degassed sealed vial was continuously recorded using an NO electrode. When the NO concentration reached a plateau in the sealed vial, a pre-degassed solution containing the IlvD [4Fe–4S] cluster was immediately injected using a gas-tight Hamilton syringe. As shown in Figure 1(B), NO was rapidly consumed by the IlvD [4Fe–4S] cluster with a half-life time of less than 30 s. In contrast, injection of a pre-degassed solution containing apo-IlvD had no effect on the NO concentration in the solution. Assuming that the initial reaction requires two molecules of NO and one molecule of the IlvD [4Fe–4S] cluster as shown in eqn (2), we estimated the rate constant for the initial reaction between NO and the IlvD [4Fe–4S] cluster to be $(7.0 \pm 2.0) \times 10^6$ $M^{-2} \cdot s^{-1}$ ($n = 4$), which is approx. 2–3 times faster than that of the NO autoxidation by O_2 in aqueous solution (2.0×10^6 $M^{-2} \cdot s^{-1}$) [3,4].

The reaction between NO and the IlvD [4Fe–4S] cluster was also traced by EPR spectroscopy and an enzyme-activity assay. Figure 1(C) shows that the EPR signal at $g = 2.04$ representing the protein-bound DNIC [22–28] quickly appeared (within 15 s) after injection of the IlvD [4Fe–4S] cluster into the NO solution anaerobically. Using glutathione-bound DNIC as a standard [30], we estimated that the maximum amount of 1.8 ± 0.5 molecules of DNIC per each IlvD [4Fe–4S] cluster were formed by NO under anaerobic conditions. The parallel enzyme activity measurements revealed that IlvD was also rapidly inactivated upon the injection to the NO solution anaerobically (Figure 1D).

To further examine the reactivity of the IlvD [4Fe–4S] cluster with NO, we injected the pre-degassed IlvD [4Fe–4S] cluster into the sealed vials containing different concentrations of NO anaerobically. After 3 min incubation, aliquots were immediately taken from the reaction solutions for the parallel EPR and enzyme-activity measurements. Figure 2 shows that, as the NO concentration was increased (from 0 to 150 μM) in the pre-

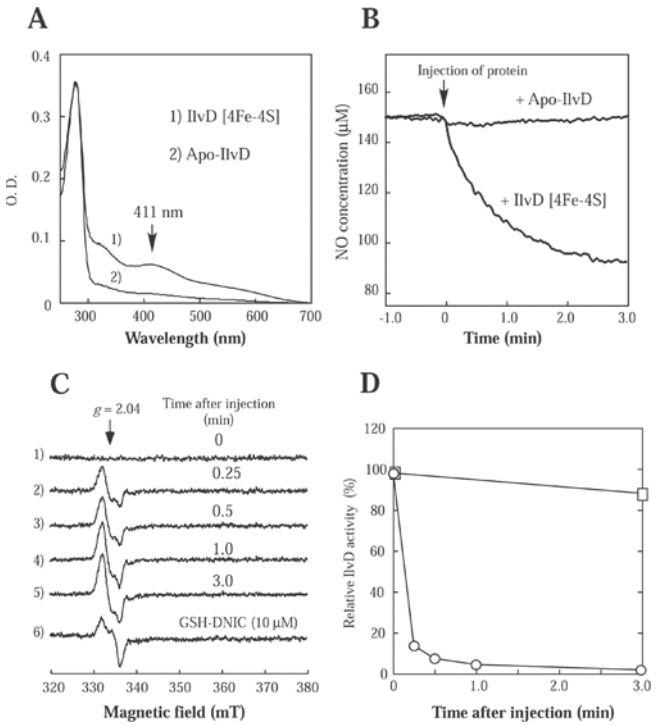

Figure 1 NO is rapidly consumed by the IlvD [4Fe–4S] cluster under anaerobic conditions

(**A**) UV–visible absorption spectra of apo-IlvD and the IlvD [4Fe–4S] cluster. Protein (10 μM) was dissolved in buffer containing 20 mM potassium phosphate (pH 7.2). (**B**) Kinetics of NO consumption by apo-IlvD and the IlvD [4Fe–4S] cluster under anaerobic conditions. Pre-degassed apo-IlvD or the IlvD [4Fe–4S] cluster (at a final concentration of 10 μM) was injected into a pre-degassed sealed vial containing NO ($\sim$150 μM) using a gas-tight syringe anaerobically. The NO concentration in the reaction solution was continuously recorded using an NO electrode. Injection of an equal volume of pre-degassed phosphate buffer to the NO solution was used as a reference. (**C**) Formation of the IlvD-bound DNIC by NO. For the EPR spectra (1–5), the IlvD samples were taken from the reaction solution at 0, 0.25, 0.5, 1 and 3 min after the IlvD [4Fe–4S] cluster was injected into the NO solution anaerobically. Spectrum 6 was the freshly prepared GSH-bound DNIC (10 μM). (**D**) Inactivation of IlvD by NO under anaerobic conditions. The enzyme activity of IlvD was measured as described in the Experimental section. Aliquots were taken from the reaction solution at the indicated time points after the IlvD [4Fe–4S] cluster was injected into the NO solution anaerobically. ○, The relative enzyme activities after the IlvD [4Fe–4S] cluster was injected into the NO solution. □, the relative enzyme activities of IlvD not treated with NO. The results are representative of three independent experiments.

incubated solution, the amount of the IlvD-bound DNIC was gradually increased (Figure 2A) and the enzyme activity of IlvD was progressively decreased (Figure 2B). Taken together, the results demonstrated that NO can directly and efficiently react with the IlvD [4Fe–4S] cluster forming the IlvD-bound DNIC and inactivate the enzyme activity of IlvD under anaerobic conditions.

Effect of O_2 on the NO-mediated modification of the IlvD [4Fe–4S] cluster

The observed rate constant for the initial reaction between NO and the IlvD [4Fe–4S] cluster (Figure 1B) indicates that NO could be more reactive with the IlvD [4Fe–4S] cluster than with O_2. To directly compare the relative reactivity of NO with the IlvD [4Fe–4S] cluster and O_2, we measured the NO consumption kinetics by O_2 and the IlvD [4Fe–4S] cluster. Figure 3(A) shows that the NO consumption was evidently faster by the IlvD [4Fe–4S] cluster (10 μM) than by O_2 (10 μM). When equal amounts of the IlvD [4Fe–4S] cluster and O_2 were injected together

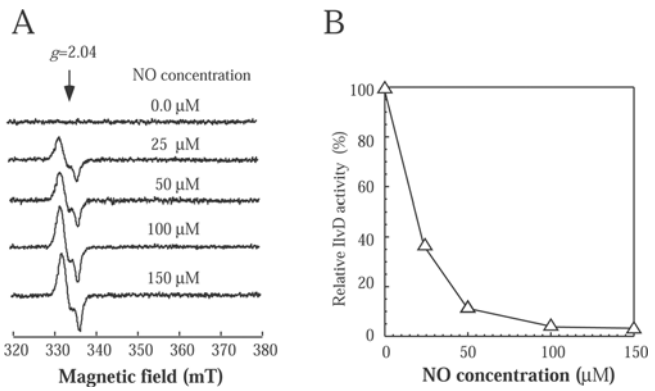

Figure 2 Sensitivity of the IlvD [4Fe–4S] cluster to NO

Purified IlvD [4Fe–4S] cluster (at a final concentration of 10 μM) was injected into a pre-degassed sealed vial containing 0, 25, 50, 100 and 150 μM NO using a gas-tight syringe anaerobically. After 3 min incubation, aliquots were taken for the EPR and enzyme-activity measurements. (**A**) The EPR spectra of IlvD after injection into the NO solutions for 3 min. (**B**) The relative enzyme activities of IlvD after injection into the NO solutions for 3 min. The experiments were repeated three times, and similar results were obtained.

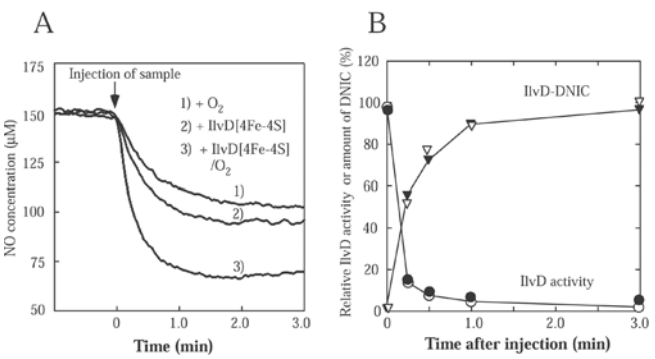

Figure 3 Relative reactivity of NO with the IlvD [4Fe–4S] cluster and O_2

(**A**) Kinetics of NO consumption by the IlvD [4Fe–4S] cluster and O_2. Pre-degassed IlvD [4Fe–4S] cluster or O_2 (at a final concentration of 10 μM) was either injected individually or together into a pre-degassed sealed vial containing NO solution (~150 μM) anaerobically. The NO concentration in the reaction solution was continuously recorded using an NO electrode. (**B**) Formation of the IlvD-bound DNIC and inactivation of the enzyme activity by NO. The amounts of the IlvD-bound DNIC after injection into the NO solution with (▼) or without (▽) 10 μM O_2. The relative enzyme activities of IlvD after injection into the NO solution with (●) or without (○) 10 μM O_2. The results are representative of at least three experiments.

into the NO solution, the NO consumption became even faster (Figure 3A), indicating that both the IlvD [4Fe–4S] cluster and O_2 may simultaneously consume NO. Attempts were made to deconvolute the observed kinetics of the NO consumption by the IlvD [4Fe–4S] cluster and O_2 in the solutions. However, simple algorithms were not sufficient to simulate the NO consumption, probably because the reaction becomes more complex after initial steps (see the Discussion below).

To examine whether the IlvD [4Fe–4S] cluster was modified forming the IlvD-bound DNIC by NO in the presence of O_2, we again followed the reaction by EPR spectroscopy and enzyme activity measurements. Figure 3(B) shows that the IlvD-bound DNIC was quickly formed with the concomitant inactivation of the enzyme activity when both the IlvD [4Fe–4S] cluster and O_2 were injected into the NO solution. The nearly identical kinetics for the formation of the IlvD-bound DNIC and inactivation of the IlvD activity by NO in the absence and presence of O_2 suggested that NO has a higher reactivity with the IlvD [4Fe–4S] cluster than with O_2 in solution.

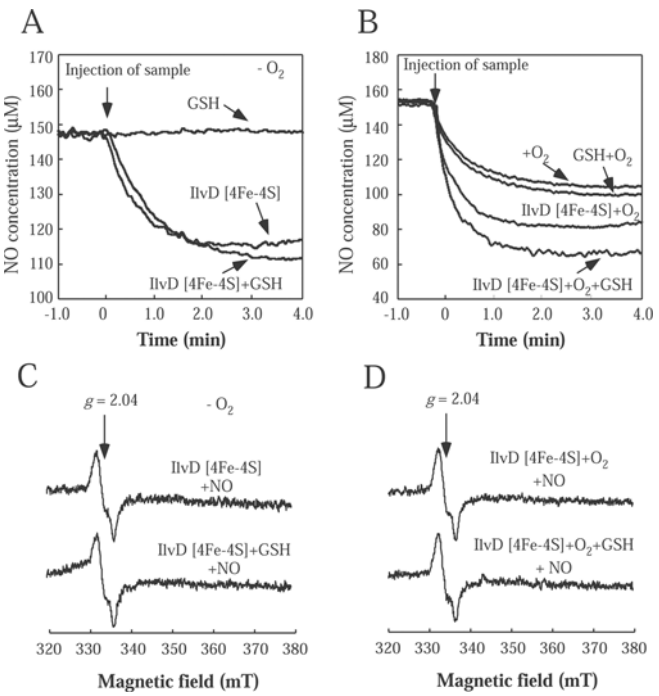

Figure 4 GSH fails to protect the IlvD [4Fe–4S] cluster from being modified by NO with or without O_2

(**A**) Kinetics of NO consumption by GSH and the IlvD [4Fe–4S] cluster under anaerobic conditions. Pre-degassed GSH (at a final concentration of 1 mM) or the IlvD [4Fe–4S] cluster (at a final concentration of 10 μM) was injected individually or together into a pre-degassed sealed vial containing NO solution (~150 μM) anaerobically. The NO concentration in the reaction solution was continuously recorded with an NO electrode. (**B**) The NO consumption by GSH and the IlvD [4Fe–4S] cluster in the presence of O_2. Aerated GSH (1 mM) or the IlvD [4Fe–4S] cluster (10 μM) was injected individually or together into a pre-degassed sealed vial containing NO solution (~150 μM). The NO concentration in the reaction solution was continuously recorded with an NO electrode. (**C**) The EPR spectra of IlvD after injection into the NO solution with or without GSH anaerobically. (**D**) The EPR spectra of IlvD after injection into the NO solution with or without GSH in the presence of O_2 (10 μM). The EPR samples were taken 3 min after injection of the protein into the NO solution.

Small molecule thiol GSH fails to protect the IlvD [4Fe–4S] cluster from being modified by NO under aerobic and anaerobic conditions

Small molecule thiols are abundant in cells [42], and have an important defensive role against NO cytotoxicity [33]. To test whether small molecule thiols can protect the NO-mediated modification of iron–sulfur clusters, in the present study we used GSH as an example. Figure 4(A) shows that injection of pre-degassed GSH (1 mM) did not consume NO under anaerobic conditions, consistent with the notion that NO does not directly react with small molecule thiols without O_2 [42]. When a pre-degassed solution containing 1 mM GSH and 10 μM IlvD [4Fe–4S] cluster was injected into the NO solution anaerobically, the NO consumption was essentially identical with that when only 10 μM IlvD [4Fe–4S] cluster was injected (Figure 4A). The EPR measurements further revealed that the IlvD [4Fe–4S] cluster was modified forming the IlvD-bound DNIC by NO regardless of the presence of GSH (Figure 4C). In parallel, the enzyme-activity measurements showed that GSH failed to prevent the inactivation of IlvD by NO (results not shown). Thus GSH has little or no protective effect on the NO-mediated modification of the IlvD [4Fe–4S] cluster under anaerobic conditions.

Under aerobic conditions, GSH can be converted into GSNO (*S*-nitrosoglutathione) by NO via a mechanism possibly mediated by NO_2 and the subsequent reaction of thiyl radicals with NO [42].

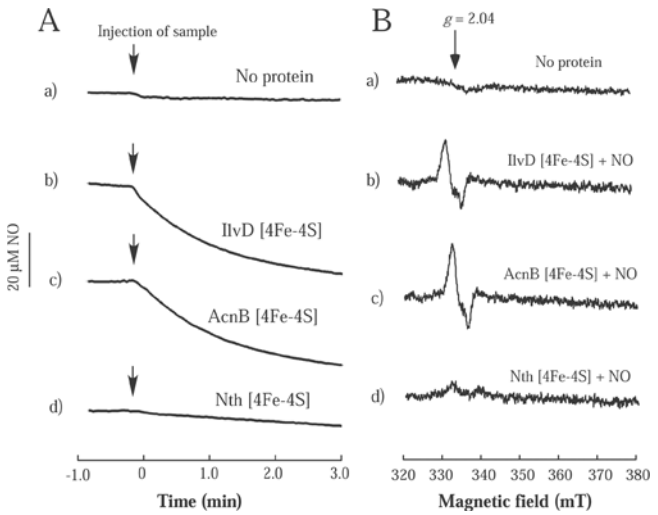

Figure 5 Reactivity of NO with different iron–sulfur proteins under anaerobic conditions

(**A**) Kinetics of NO consumption by buffer only (a), the IlvD [4Fe–4S] cluster (b), the aconitase B [4Fe–4S] cluster (c) and the endonuclease III [4Fe–4S] cluster (d). Pre-degassed protein sample (at a final concentration of 10 μM) was injected into a pre-degassed sealed vial containing NO ($\sim$150 μM) anaerobically. The NO concentration in the reaction solution was continuously recorded using an NO electrode. (**B**) The EPR spectra of the protein samples. The EPR samples were taken directly from the reaction solutions 3 min after injection into the NO solution. The results are representative of three independent experiments.

It would be pertinent to examine whether GSH can kinetically compete with the IlvD [4Fe–4S] cluster to react with NO in the presence of O_2. Figure 4(B) shows that addition of 1 mM GSH did not significantly stimulate the NO autoxidation by O_2, indicating that the reaction between GSH and NO in the presence of O_2 was relatively slow. On the other hand, addition of 1mM GSH to the mixture of 10 μM IlvD [4Fe–4S] cluster and 10 μM O_2 clearly stimulated the NO consumption kinetics. We postulated that under these conditions, O_2 and 'free' iron released from the disrupted iron–sulfur clusters may promote *S*-nitrosylation of GSH [42], thus increasing the NO consumption. The parallel EPR measurements confirmed that the IlvD [4Fe–4S] cluster was modified by NO forming the IlvD-bound DNIC regardless of the presence of GSH and O_2 (Figure 4D). The enzyme activity measurements further showed that IlvD was inactivated by NO in the presence of GSH and O_2 (results not shown). Thus GSH fails to prevent the NO-mediated modification of the IlvD [4Fe–4S] cluster in the absence or presence of O_2.

Reactivity of NO with the [4Fe–4S] cluster in other proteins

The experimental setting described above allowed us to compare the reactivity of NO with different iron–sulfur proteins. In the present study, we chose the aconitase B [4Fe–4S] cluster [43] and endonuclease III [4Fe–4S] cluster [25,44] from *E. coli* as examples. Aconitase B represents the major aconitase activity of the tricarboxylic acid cycle in *E. coli* [43,45], whereas endonuclease III is a DNA glycosylase/AP (apurinic/apyrimidinic)-endonuclease involved in the base excision repair pathway [25,44]. Both proteins were purified as described in the Experimental section. Figure 5(A) shows that the aconitase B [4Fe–4S] cluster had almost identical NO consumption kinetics as the IlvD [4Fe–4S] cluster. However, the reaction between NO with the endonuclease III [4Fe–4S] cluster was relatively slow. The EPR measurements further revealed that both the IlvD [4Fe–4S] cluster and the aconitase B [4Fe–4S] cluster were converted into the protein-bound DNIC after injection into the NO solution, whereas the amount of the endonuclease III-bound DNIC was much less after the same NO exposure (Figure 5B). A simple explanation for the different reactivity of NO with the [4Fe–4S] cluster could be the location of the cluster in proteins [46]. Structurally, the [4Fe–4S] clusters in both aconitase B [43] and IlvD [35] are highly accessible to solvent, and thus are prone to NO modification. In contrast, the [4Fe–4S] cluster in endonuclease III is largely buried within the protein structure [47], rendering it resistant to NO modification.

The IlvD [4Fe–4S] cluster is readily modified forming the IlvD-bound DNIC by NO in *E. coli* cells under both aerobic and anaerobic growth conditions

The results described above led us to propose that NO has a higher reactivity with the IlvD [4Fe–4S] cluster than with O_2 and small molecule thiol GSH. To explore the physiological relevance of this observation, we exposed the exponentially growing *E. coli* cells containing the recombinant IlvD [4Fe–4S] cluster to NO using the Silastic tubing NO-delivery system [41] under aerobic and anaerobic growth conditions. The Silastic tubing NO-delivery system allowed us to emulate the NO productions in activated macrophages or neutrophils [7,8]. When *E. coli* cells were subjected to NO exposure at a rate of 100 nM NO per s either anaerobically (Figure 6A) or aerobically (Figure 6B), the enzyme activity of the recombinant IlvD in *E. coli* cells was rapidly inactivated under both conditions. The recombinant IlvD was then purified from *E. coli* cells after different NO exposure times. The EPR measurements of purified IlvD samples demonstrated that the IlvD [4Fe–4S] cluster was efficiently converted into the IlvD-bound DNIC by NO under both anaerobic (Figure 6C) and aerobic conditions (Figure 6D). Similar results were obtained when the *E. coli* cells containing the recombinant aconitase B [4Fe–4S] cluster were exposed to NO under aerobic and anaerobic conditions (see Supplementary Figure 1 at http://www.BiochemJ.org/bj/417/bj4170783add.htm). However, the same NO exposure of the *E. coli* cells containing the recombinant endonuclease III produced only a small amount of the endonuclease III-bound DNIC (results not shown), consistent with its slow reaction kinetics with NO (Figure 5A). The results suggested that NO is highly effective in modifying the [4Fe–4S] clusters in IlvD and aconitase B in *E. coli* cells under both aerobic and anaerobic conditions.

DISCUSSION

In the present study, we report the first kinetic characterization of the reaction between NO and the [4Fe–4S] cluster of IlvD. Combining a sensitive NO electrode with EPR spectroscopy and an enzyme-activity assay, we demonstrated that NO can rapidly react with the IlvD [4Fe–4S] cluster forming the IlvD-bound DNIC and inactivate the enzyme activity under anaerobic conditions. The rate constant for the initial reaction between NO and the IlvD [4Fe–4S] cluster is approx. $(7.0 \pm 2.0) \times 10^6$ $M^{-2} \cdot s^{-1}$, which is approx. 2–3 times faster than that of the NO autoxidation by O_2 in aqueous solution. Consistent with the observed rate constant, we found that O_2 does not significantly affect the NO-mediated modification of the IlvD [4Fe–4S] cluster, and that small molecule thiol GSH fails to protect the IlvD [4Fe–4S] cluster from being modified by NO under both aerobic and anaerobic conditions *in vitro*. *In vivo* studies revealed that NO is equally effective in modifying the IlvD [4Fe–4S] cluster in *E. coli* cells

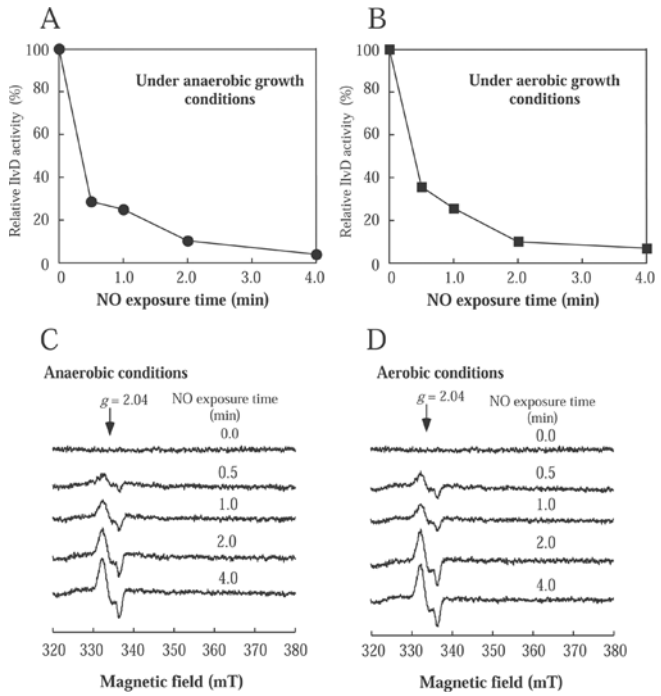

Figure 6 Modification of the IlvD [4Fe–4S] cluster by NO *in vivo* under aerobic and anaerobic growth conditions

E. coli cells expressing the recombinant IlvD [4Fe–4S] cluster were exposed to NO at a rate of 100 nM per s using the Silastic tubing NO delivery system under aerobic or anaerobic conditions. (**A**) The relative enzyme activities of the recombinant IlvD in the cell extracts prepared from the *E. coli* cells exposed to NO for the times indicated under anaerobic conditions. (**B**) The relative enzyme activities of the recombinant IlvD in the cell extracts prepared from the *E. coli* cells exposed to NO for the times indicated under aerobic conditions. The enzyme activity of IlvD in the untreated *E. coli* cells (100 %) was approx. 11.3 μmol of oxo acids formed/mg of cellular protein per min. (**C**) EPR spectra of the recombinant IlvD purified from the *E. coli* cells exposed to NO for the times indicated under anaerobic conditions. (**D**) EPR spectra of the recombinant IlvD purified from the *E. coli* cells exposed to NO for the times indicated under aerobic conditions. The concentrations of the purified IlvD in (**C**) and (**D**) were calibrated to be approx. 10 μM.

under aerobic and anaerobic growth conditions, confirming that NO has a higher reactivity with the IlvD [4Fe–4S] cluster than with O_2 and GSH. The results led us to propose that the iron–sulfur clusters in proteins such as IlvD may constitute the primary targets of NO cytotoxicity under both anaerobic and aerobic conditions.

The NO-mediated modification of iron–sulfur proteins has been well documented in bacteria and mammalian cells [17–28]. Using synthetic model compounds, the possible reactivity pathways for NO with iron–sulfur clusters have also been proposed [48–50]; however, to the best of our knowledge, the reaction kinetics between NO and iron–sulfur clusters in proteins have never been reported. Considering that there are numerous potential targets of NO in cells, it is imperative to determine the specific reactivity of NO with these targets. In the present study, we reported that NO can directly and efficiently react with the IlvD [4Fe–4S] cluster *in vitro* and *in vivo*, and that the major product of the reaction is the IlvD-bound DNIC. Nevertheless, we were unable to simulate the observed kinetics of the NO consumption using simple algorithms, as the redox reactions underlying the NO-mediated modifications of iron–sulfur clusters are still not fully understood. In addition, the iron and sulfide released from the disrupted iron–sulfur clusters could potentially react with NO, thus further complicating the NO consumption kinetics in the reaction (Figure 1B). Although our results clearly suggested that iron–sulfur clusters are the primary targets of NO cytotoxicity, it should be pointed out that not all iron–sulfur proteins have the same reactivity with NO. Whereas the aconitase B [4Fe–4S] cluster has an almost identical NO reactivity as the IlvD [4Fe–4S] cluster *in vitro* and *in vivo*, the reaction between NO and the endonuclease III [4Fe–4S] cluster is relatively slow (Figure 5). We attributed the different reactivity of iron–sulfur clusters with NO to their solvent accessibility in proteins as suggested previously by Varghese et al. [43].

In biological systems, O_2 is the major factor that determines the half-life time of NO, as NO can be quickly autoxidized by O_2 at a rate constant of 2.0×10^6 $M^{-2} \cdot s^{-1}$ at 25 °C [3,4]. Another major cellular factor that may limit the NO availability is small molecule thiols [33]. Under aerobic conditions, small molecule thiols can be converted into *S*-nitrosothiols by NO via a mechanism involving formation of NO_2 and the subsequent reaction of thiyl radicals with NO [33,42]. Nevertheless, despite the presence of O_2 and abundant small molecule thiols in cells, NO can still act as an efficient signalling molecule in neuronal and cardiovascular tissues [10,11] and as a potent inhibitor of the respiratory electron-transfer chain in mitochondria [13,14]. This is largely due to the high binding affinity of NO to haems in proteins [10,11]. The results of the present study demonstrated that NO also has a higher reactivity with the [4Fe–4S] cluster in IlvD and aconitase B than with O_2 and small molecule thiol GSH, as addition of 100-fold excess of GSH fails to prevent the NO-mediated modification of the IlvD [4Fe–4S] cluster in the presence or absence of O_2 (Figure 4). This notion is further confirmed by the *in vivo* studies showing that NO at pathophysiological concentrations [7,8] is equally effective in converting the IlvD [4Fe–4S] cluster into the IlvD-bound DNIC in *E. coli* cells under aerobic and anaerobic conditions (Figure 6). Thus iron–sulfur clusters, like haems, are the preferred targets of NO cytotoxicity under anaerobic and aerobic conditions.

NO is considered an effective anti-bacterial and anti-tumour cytotoxic agent [7–9]. Unlike reversible binding of NO to haems in soluble guanylate cyclase [11] or the binuclear haem a_3/Cu_B centre in cytochrome *c* oxidase [12–14], the reaction of NO with iron–sulfur clusters is irreversible with the concomitant formation of the protein-bound DNIC [22–28,38] (Figure 1). Since iron–sulfur proteins are broadly distributed [16,38], modification of iron–sulfur clusters by NO is expected to inactivate multiple physiological processes. If cells are to survive, the NO-modified iron–sulfur clusters must be efficiently repaired. The cellular repair mechanisms for the NO-modified iron–sulfur clusters are currently under investigation.

FUNDING

This work was supported by the National Institutes of Health [grant number CA107494] (Public Health Service Grant to H. D.)

REFERENCES

1 Thomas, D. D., Liu, X., Kantrow, S. P. and Lancaster, Jr, J. R. (2001) The biological lifetime of nitric oxide: implications for the perivascular dynamics of NO and O_2. Proc. Natl. Acad. Sci. U.S.A. **98**, 355–360
2 Stamler, J. S., Singel, D. J. and Loscalzo, J. (1992) Biochemistry of nitric oxide and its redox-activated forms. Science **258**, 1898–1902
3 Ford, P. C., Wink, D. A. and Stanbury, D. M. (1993) Autoxidation kinetics of aqueous nitric oxide. FEBS Lett. **326**, 1–3
4 Liu, X., Miller, M. J., Joshi, M. S., Thomas, D. D. and Lancaster, Jr, J. R. (1998) Accelerated reaction of nitric oxide with O_2 within the hydrophobic interior of biological membranes. Proc. Natl. Acad. Sci. U.S.A. **95**, 2175–2179
5 Shiva, S., Brookes, P. S., Patel, R. P., Anderson, P. G. and Darley-Usmar, V. M. (2001) Nitric oxide partitioning into mitochondrial membranes and the control of respiration at cytochrome *c* oxidase. Proc. Natl. Acad. Sci. U.S.A. **98**, 7212–7217

6 Ignarro, L. J. (1999) Nitric oxide: a unique endogenous signaling molecule in vascular biology. Biosci. Rep. **19**, 51–71
7 Krieglstein, C. F., Cerwinka, W. H., Laroux, F. S., Salter, J. W., Russell, J. M., Schuermann, G., Grisham, M. B., Ross, C. R. and Granger, D. N. (2001) Regulation of murine intestinal inflammation by reactive metabolites of oxygen and nitrogen: divergent roles of superoxide and nitric oxide. J. Exp. Med. **194**, 1207–1218
8 Gobert, A. P., McGee, D. J., Akhtar, M., Mendz, G. L., Newton, J. C., Cheng, Y., Mobley, H. L. and Wilson, K. T. (2001) *Helicobacter pylori* arginase inhibits nitric oxide production by eukaryotic cells: a strategy for bacterial survival. Proc. Natl. Acad. Sci. U.S.A. **98**, 13844–13849
9 MacMicking, J., Xie, Q. W. and Nathan, C. (1997) Nitric oxide and macrophage function. Annu. Rev. Immunol. **15**, 323–350
10 Scheele, J. S., Bruner, E., Kharitonov, V. G., Martasek, P., Roman, L. J., Masters, B. S., Sharma, V. S. and Magde, D. (1999) Kinetics of NO ligation with nitric-oxide synthase by flash photolysis and stopped-flow spectrophotometry. J. Biol. Chem. **274**, 13105–13110
11 Kharitonov, V. G., Sharma, V. S., Magde, D. and Koesling, D. (1999) Kinetics and equilibria of soluble guanylate cyclase ligation by CO: effect of YC-1. Biochemistry **38**, 10699–10706
12 Koivisto, A., Matthias, A., Bronnikov, G. and Nedergaard, J. (1997) Kinetics of the inhibition of mitochondrial respiration by NO. FEBS Lett. **417**, 75–80
13 Cleeter, M. W., Cooper, J. M., Darley-Usmar, V. M., Moncada, S. and Schapira, A. H. (1994) Reversible inhibition of cytochrome *c* oxidase, the terminal enzyme of the mitochondrial respiratory chain, by nitric oxide. Implications for neurodegenerative diseases. FEBS Lett. **345**, 50–54
14 Brookes, P. S., Kraus, D. W., Shiva, S., Doeller, J. E., Barone, M. C., Patel, R. P., Lancaster, Jr, J. R. and Darley-Usmar, V. (2003) Control of mitochondrial respiration by NO*, effects of low oxygen and respiratory state. J. Biol. Chem. **278**, 31603–31609
15 Spiro, S. (2007) Regulators of bacterial responses to nitric oxide. FEMS Microbiol. Rev. **31**, 193–211
16 Johnson, D. C., Dean, D. R., Smith, A. D. and Johnson, M. K. (2005) Structure, function, and formation of biological iron–sulfur clusters. Annu. Rev. Biochem. **74**, 247–281
17 Reddy, D., Lancaster, Jr, J. R. and Cornforth, D. P. (1983) Nitrite inhibition of *Clostridium botulinum*: electron spin resonance detection of iron–nitric oxide complexes. Science **221**, 769–770
18 Lancaster, Jr, J. R. and Hibbs, Jr, J. B. (1990) EPR demonstration of iron–nitrosyl complex formation by cytotoxic activated macrophages. Proc. Natl. Acad. Sci. U.S.A. **87**, 1223–1227
19 Drapier, J. C., Pellat, C. and Henry, Y. (1991) Generation of EPR-detectable nitrosyl–iron complexes in tumor target cells cocultured with activated macrophages. J. Biol. Chem. **266**, 10162–10167
20 Pieper, G. M., Halligan, N. L., Hilton, G., Konorev, E. A., Felix, C. C., Roza, A. M., Adams, M. B. and Griffith, O. W. (2003) Non-heme iron protein: a potential target of nitric oxide in acute cardiac allograft rejection. Proc. Natl. Acad. Sci. U.S.A. **100**, 3125–3130
21 Asanuma, K., Iijima, K., Ara, N., Koike, T., Yoshitake, J., Ohara, S., Shimosegawa, T. and Yoshimura, T. (2007) Fe–S cluster proteins are intracellular targets for nitric oxide generated luminally at the gastro-oesophageal junction. Nitric Oxide **16**, 395–402
22 Kennedy, M. C., Antholine, W. E. and Beinert, H. (1997) An EPR investigation of the products of the reaction of cytosolic and mitochondrial aconitases with nitric oxide. J. Biol. Chem. **272**, 20340–20347
23 Foster, M. W. and Cowan, J. A. (1999) Chemistry of nitric oxide with protein-bound iron sulfur centers. Insights on physiological reactivity. J. Am. Chem. Soc. **121**, 4093–4100
24 Drapier, J. C. (1997) Interplay between NO and [Fe–S] clusters: relevance to biological systems. Methods **11**, 319–329
25 Rogers, P. A., Eide, L., Klungland, A. and Ding, H. (2003) Reversible inactivation of *E. coli* endonuclease III by nitric oxide via modification of its [4Fe–4S] cluster. DNA Repair **2**, 809–817
26 Ding, H. and Demple, B. (2000) Direct nitric oxide signal transduction via nitrosylation of iron–sulfur centers in the SoxR transcription activator. Proc. Natl. Acad. Sci. U.S.A. **97**, 5146–5150
27 Cruz-Ramos, H., Crack, J., Wu, G., Hughes, M. N., Scott, C., Thomson, A. J., Green, J. and Poole, R. K. (2002) NO sensing by FNR: regulation of the *Escherichia coli* NO-detoxifying flavohaemoglobin, Hmp. EMBO J. **21**, 3235–3244
28 Rogers, P. A. and Ding, H. (2001) L-Cysteine-mediated destabilization of dinitrosyl iron complexes in proteins. J. Biol. Chem. **276**, 30980–30986
29 Vanin, A. F., Malenkova, I. V., Mordvintsev, O. I. and Miul'sh, A. (1993) Dinitrosyl complexes of iron with thiol-containing ligands and their reverse conversion into nitrosothiols. Biokhimiia **58**, 1094–1103
30 Vanin, A. F. (1998) Dinitrosyl iron complexes and *S*-nitrosothiols are two possible forms for stabilization and transport of nitric oxide in biological systems. Biochemistry (Mosc.) **63**, 782–793
31 Butler, A. R. and Megson, I. L. (2002) Non-heme iron nitrosyls in biology. Chem. Rev. **102**, 1155–1166
32 Ueno, T. and Yoshimura, T. (2000) The physiological activity and *in vivo* distribution of dinitrosyl dithiolato iron complex. Jpn. J. Pharmacol. **82**, 95–101
33 Pedersen, J. Z., De Maria, F., Turella, P., Federici, G., Mattei, M., Fabrini, R., Dawood, K. F., Massimi, M., Caccuri, A. M. and Ricci, G. (2007) Glutathione transferases sequester toxic dinitrosyl–iron complexes in cells. A protection mechanism against excess nitric oxide. J. Biol. Chem. **282**, 6364–6371
34 Beinert, H., Holm, R. H. and Munck, E. (1997) Iron–sulfur clusters: nature's modular, multipurpose structures. Science **277**, 653–659
35 Flint, D. H., Emptage, M. H., Finnegan, M. G., Fu, W. and Johnson, M. K. (1993) The role and properties of the iron–sulfur cluster in *Escherichia coli* dihydroxy-acid dehydratase. J. Biol. Chem. **268**, 14732–14742
36 Flint, D. H., Smyk-Randall, E., Tuminello, J. F., Draczynska-Lusiak, B. and Brown, O. R. (1993) The inactivation of dihydroxy-acid dehydratase in *Escherichia coli* treated with hyperbaric oxygen occurs because of the destruction of its Fe–S cluster, but the enzyme remains in the cell in a form that can be reactivated. J. Biol. Chem. **268**, 25547–25552
37 Hyduke, D. R., Jarboe, L. R., Tran, L. M., Chou, K. J. and Liao, J. C. (2007) Integrated network analysis identifies nitric oxide response networks and dihydroxyacid dehydratase as a crucial target in *Escherichia coli*. Proc. Natl. Acad. Sci. U.S.A. **104**, 8484–8489
38 Ren, B., Zhang, N., Yang, J. and Ding, H. (2008) Nitric oxide-induced bacteriostasis and modification of iron–sulfur proteins in *Escherichia coli*. Mol. Microbiol. **70**, 953–964
39 Cioffi, E. A., Shaw, K. J., Bailey, W. F. and Berg, C. M. (1980) Improved synthesis of the sodium salt of DL-α,β-dihydroxyisovaleric acid. Anal. Biochem. **104**, 485–488
40 Henson, C. P. and Cleland, W. W. (1967) Purification and kinetic studies of beef liver cytoplasmic aconitase. J. Biol. Chem. **242**, 3833–3838
41 Tamir, S., Lewis, R. S., de Rojas Walker, T., Deen, W. M., Wishnok, J. S. and Tannenbaum, S. R. (1993) The influence of delivery rate on the chemistry and biological effects of nitric oxide. Chem. Res. Toxicol. **6**, 895–899
42 Jourd'heuil, D., Jourd'heuil, F. L. and Feelisch, M. (2003) Oxidation and nitrosation of thiols at low micromolar exposure to nitric oxide. Evidence for a free radical mechanism. J. Biol. Chem. **278**, 15720–15726
43 Varghese, S., Tang, Y. and Imlay, J. A. (2003) Contrasting sensitivities of *Escherichia coli* aconitases A and B to oxidation and iron depletion. J. Bacteriol. **185**, 221–230
44 Cunningham, R. P., Asahara, H., Bank, J. F., Scholes, C. P., Salerno, J. C., Surerus, K., Munck, E., McCracken, J., Peisach, J. and Emptage, M. H. (1989) Endonuclease III is an iron–sulfur protein. Biochemistry **28**, 4450–4455
45 Gruer, M. J. and Guest, J. R. (1994) Two genetically-distinct and differentially-regulated aconitases (AcnA and AcnB) in *Escherichia coli*. Microbiology **140**, 2531–2541
46 Keyer, K. and Imlay, J. A. (1997) Inactivation of dehydratase [4Fe–4S] clusters and disruption of iron homeostasis upon cell exposure to peroxynitrite. J. Biol. Chem. **272**, 27652–27659
47 Kuo, C. F., McRee, D. E., Fisher, C. L., O'Handley, S. F., Cunningham, R. P. and Tainer, J. A. (1992) Atomic structure of the DNA repair [4Fe–4S] enzyme endonuclease III. Science **258**, 434–440
48 Harrop, T. C., Song, D. and Lippard, S. J. (2007) Reactivity pathways for nitric oxide and nitrosonium with iron complexes in biologically relevant sulfur coordination spheres. J. Inorg. Biochem. **101**, 1730–1738
49 Chiang, C. Y. and Darensbourg, M. Y. (2006) Iron nitrosyl complexes as models for biological nitric oxide transfer reagents. J. Biol. Inorg. Chem. **11**, 359–370
50 Tsai, F. T., Chiou, S. J., Tsai, M. C., Tsai, M. L., Huang, H. W., Chiang, M. H. and Liaw, W. F. (2005) Dinitrosyl iron complexes (DNICs) [L(2)Fe(NO)2]-(L=thiolate): interconversion among $(Fe(NO)_2)_9$ DNICs, $(Fe(NO)_2)_{10}$ DNICs, and [2Fe–2S] clusters, and the critical role of the thiolate ligands in regulating NO release of DNICs. Inorg. Chem. **44**, 5872–5881

Received 11 July 2008/6 October 2008; accepted 22 October 2008
Published as BJ Immediate Publication 22 October 2008, doi:10.1042/BJ20081423

Biochem. J. (2009) **417**, 783–789 (Printed in Great Britain) doi:10.1042/BJ20081423

online data

SUPPLEMENTARY ONLINE DATA

Reactivity of nitric oxide with the [4Fe–4S] cluster of dihydroxyacid dehydratase from *Escherichia coli*

Xuewu DUAN, Juanjuan YANG, Binbin REN, Guoqiang TAN and Huangen DING[1]

Department of Biological Sciences, Louisiana State University, Baton Rouge, LA 70803, U.S.A.

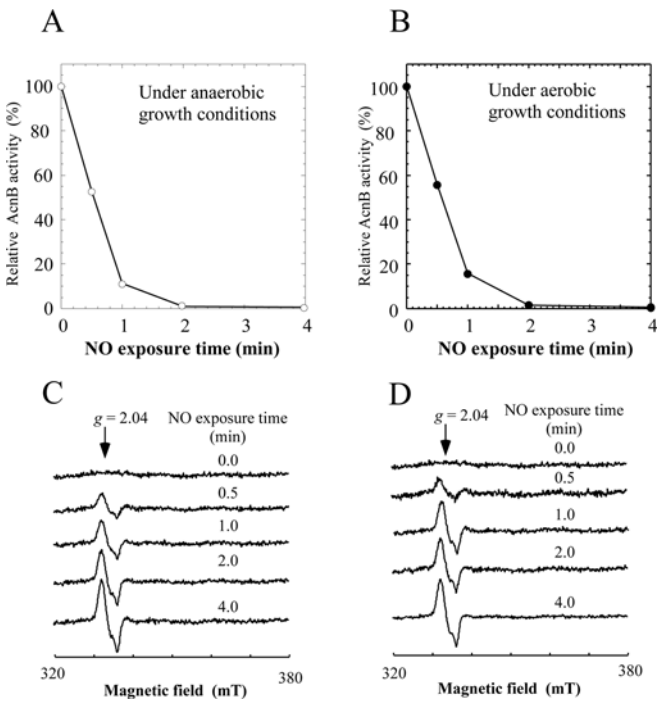

Figure S1 Modification of the aconitase B [4Fe–4S] cluster by NO *in vivo* under aerobic and anaerobic growth conditions

Escherichia coli cells expressing recombinant aconitase B [4Fe–4S] cluster were exposed to NO at a rate of 100 nM per s using the Silastic tubing NO delivery system under aerobic or anaerobic conditions. (**A**) The relative enzyme activities of recombinant aconitase B in the cell extracts prepared from the *E. coli* cells exposed to NO for the times indicated under anaerobic conditions. (**B**) The relative enzyme activities of recombinant aconitase B in the cell extracts prepared from the *E. coli* cells exposed to NO for the times indicated under aerobic conditions. (**C**) EPR spectra of recombinant aconitase B purified from the *E. coli* cells exposed to NO for the times indicated under anaerobic conditions. (**D**) EPR spectra of recombinant aconitase B purified from the *E. coli* cells exposed to NO for the times indicated under aerobic conditions. The concentrations of purified aconitase B in (**C**) and (**D**) were calibrated to be approx. 10 μM.

Received 11 July 2008/6 October 2008; accepted 22 October 2008
Published as BJ Immediate Publication 22 October 2008, doi:10.1042/BJ20081423

[1] To whom correspondence should be addressed (email hding@lsu.edu).